

# Supporting Information

## Combinatorial and rational synthesis of complex, base-modified aptamer libraries on microarrays

*Erika Schaudy<sup>a</sup>, Jory Lietard<sup>a</sup>*

<sup>a</sup>Institute of Inorganic Chemistry, University of Vienna, Vienna 1090, Austria

### Table of Contents

Determination of coupling efficiency .....	2
Determination of photolysis efficiency.....	2
RNA probe hybridization and melting.....	3
25mer probe hybridization .....	4
Aptamer target binding comparison .....	5
Modifications in St-2-1.....	6
dU-Tyr in bulge and loop of St-23-2 .....	7

# Determination of coupling efficiency

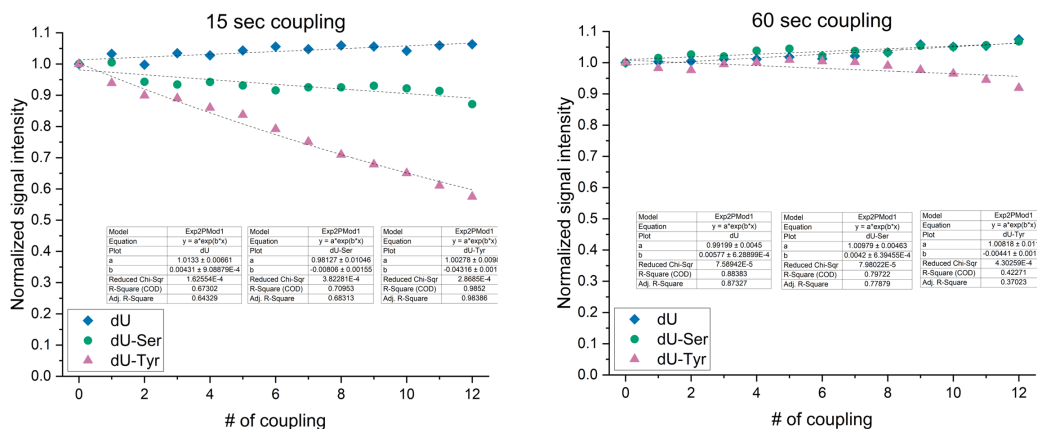


**Figure S1.** Impact of coupling time on the stepwise coupling efficiency of dU, dU-Ser and dU-Tyr phosphoramidites, comparing a reaction time of 15 seconds (left) and 60 seconds (right).

# Determination of photolysis efficiency

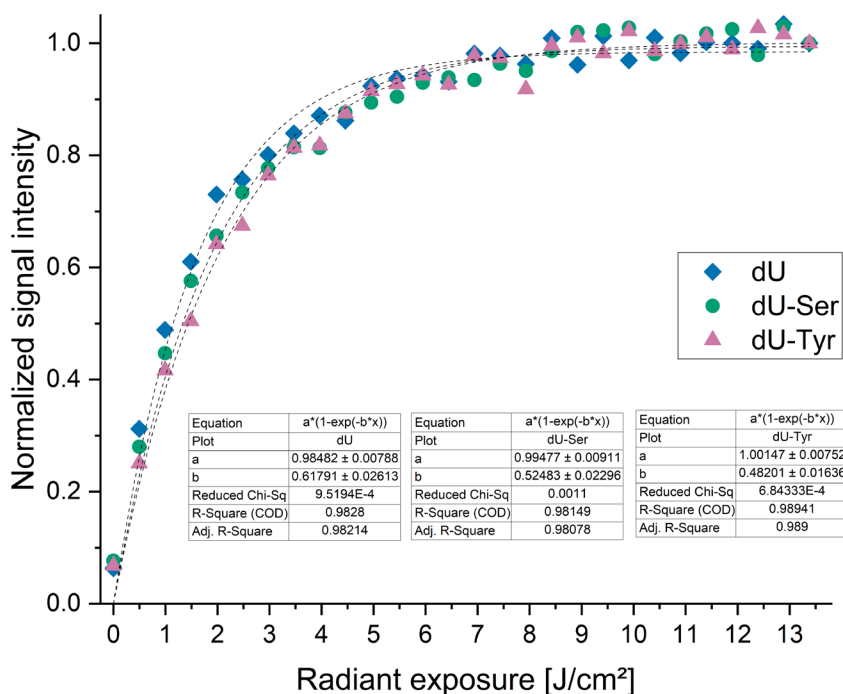


**Figure S2.** Evaluation of photolysis efficiency based on terminal labelling. An exponential model function ( $y = a \cdot (1 - e^{-bx})$ ) was fit to the data to estimate the light dose required for 95% photodeprotection of the NPPOC-protected phosphoramidites (~5.4 J/cm<sup>2</sup> for dU, ~5.9 J/cm<sup>2</sup> for dU-Ser, ~6.2 J/cm<sup>2</sup> for dU-Tyr).

# RNA probe hybridization and melting

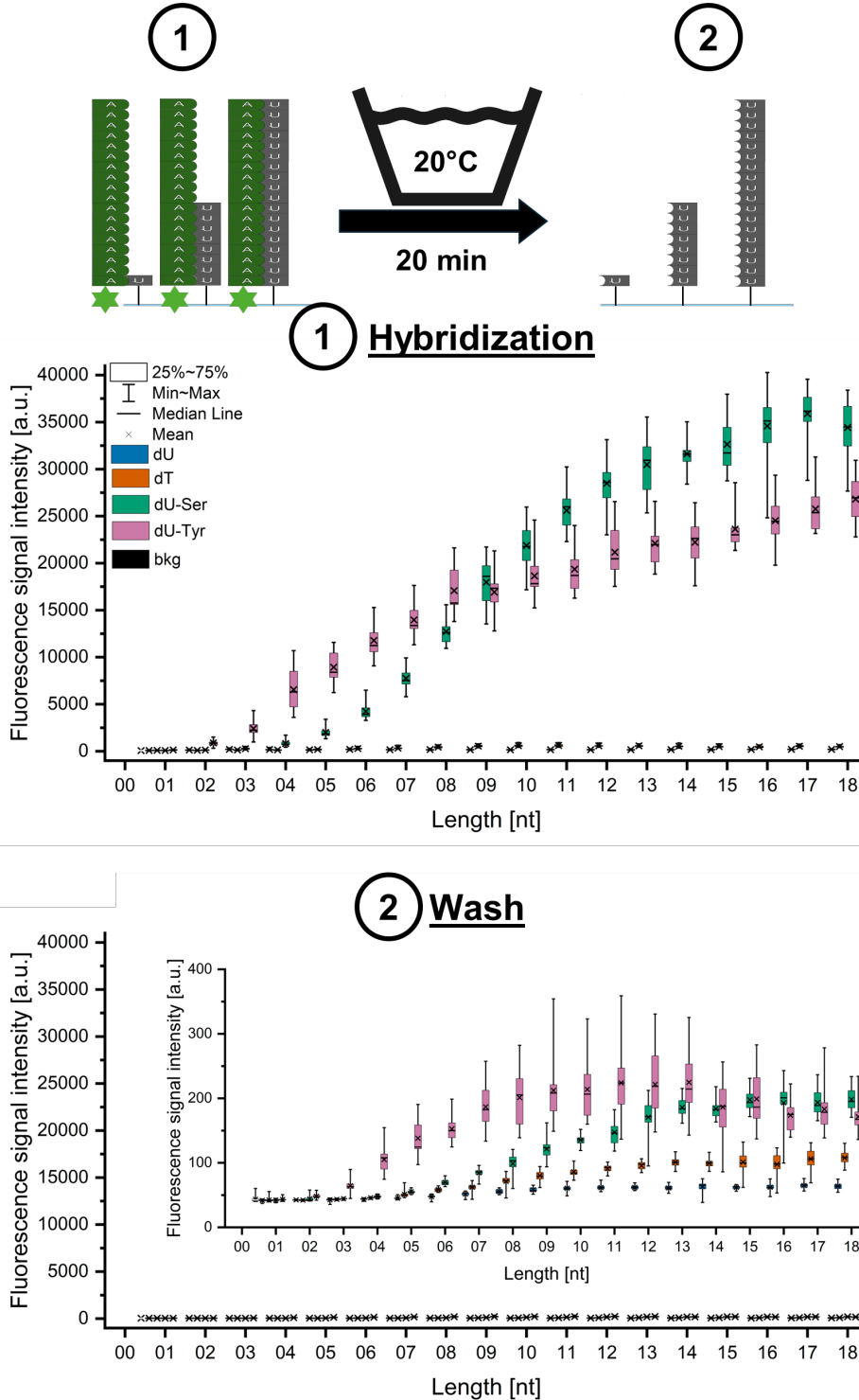


**Figure S3.** Data and schematic representation for (1) hybridization with a complementary Cy3-labeled RNA probe to a microarray with 1-18mers of dU, dT, dU-Ser and dU-Tyr, followed by 20 min wash with water at room temperature (2), including an insert with adjusted y axis to illustrate minor differences in signal intensities close to background level.

## 25mer probe hybridization

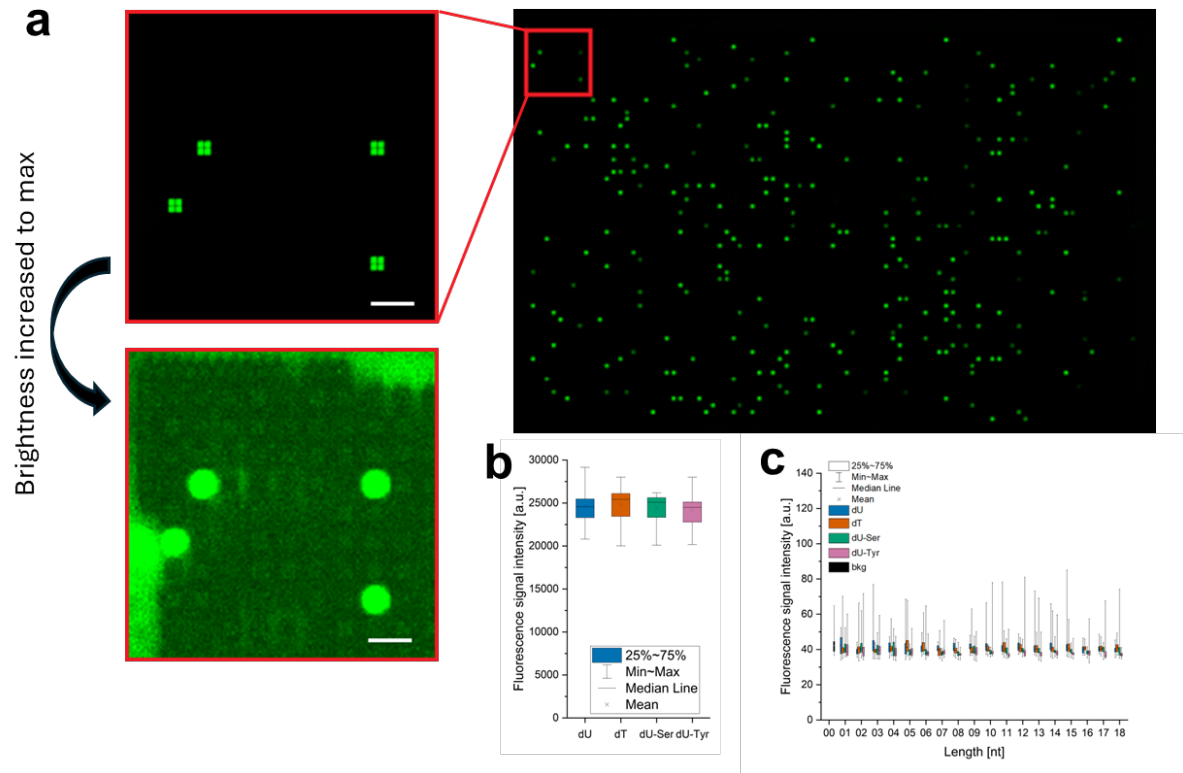


**Figure S4.** Hybridization with a Cy3-labeled mixed-nucleotide 25mer DNA probe to a microarray with complementary sequences (complementary base to all A in probe either U, T, U-Ser or U-Tyr) and 1-18 nt long homopolymer strands of dU/dT/dU-Ser/dU-Tyr. a) The scan and its excerpt (~1.5% of microarray, scale bar = 100  $\mu\text{m}$ ) of the microarray after hybridization, with extracted signal intensity data for the 25mer (b) and the 1-18mers (c) highlight both successful hybridization to the surface-bound complements independent of the dU variant present in the 25mer, and the absence of any nonspecific binding interactions with C5-modified nucleotide strands of different length.

## Aptamer target binding comparison

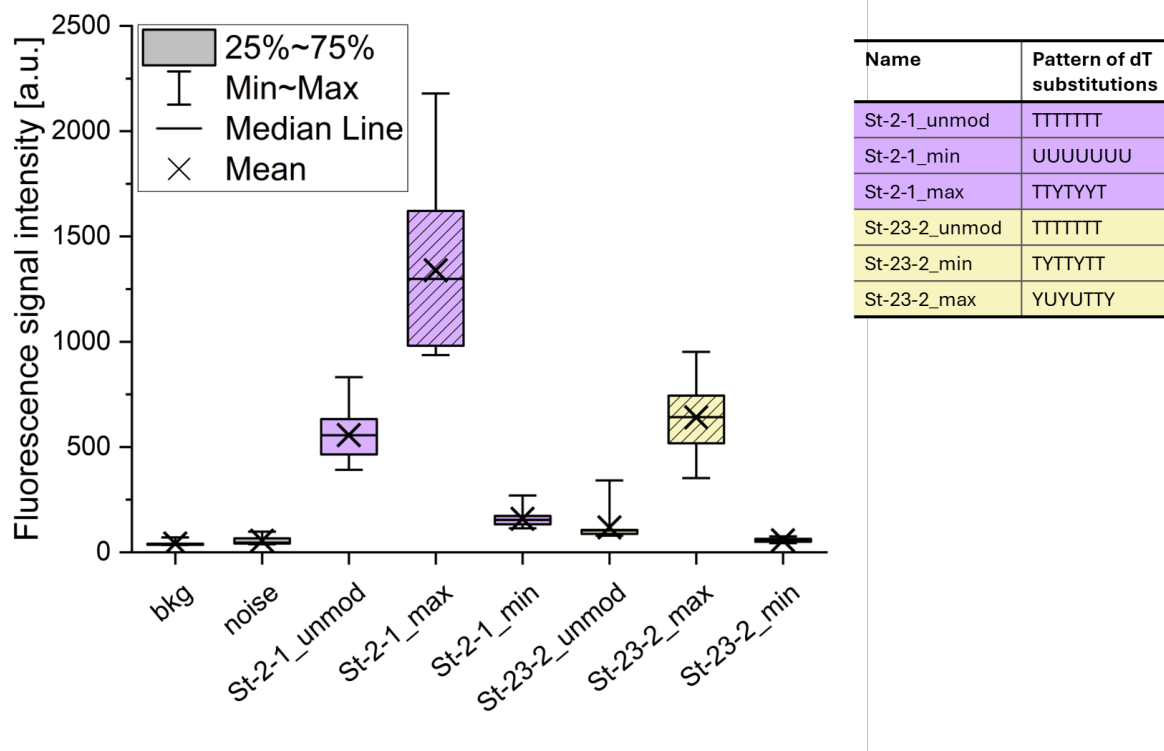


**Figure S5.** Direct comparison of the two streptavidin aptamers St-2-1 and St-2-3-2 with their sequences as published (“unmod”) and with a selected set of combinations of dU derivatives highlights the base modification’s impact on target binding, as indicated by a substantial change in detected fluorescence signal (data shown for sequence variants yielding highest – “max” – and lowest – “min” – signal). Signal-to-noise ratio is ~12, signal-to-background ratio ~14, based on the comparison with unmodified St-2-1.

## Modifications in St-2-1

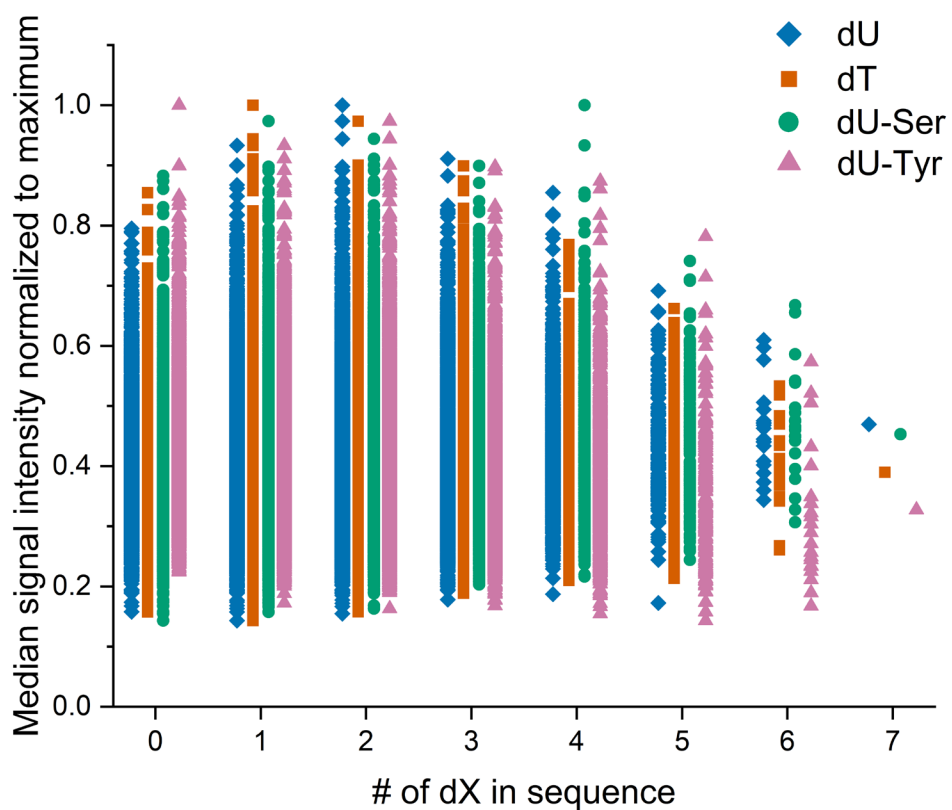


**Figure S6.** Relation of number of substitutions within the St-2-1 aptamer sequence (substitution of seven dT in the unmodified sequence with either dU, dU-Ser or dU-Tyr, yielding a permutation library of 16,384 variants) and the median fluorescence signal intensity for aptamer binding when applying 100 nM Cy3-labeled streptavidin.

## dU-Tyr in bulge and loop of St-23-2

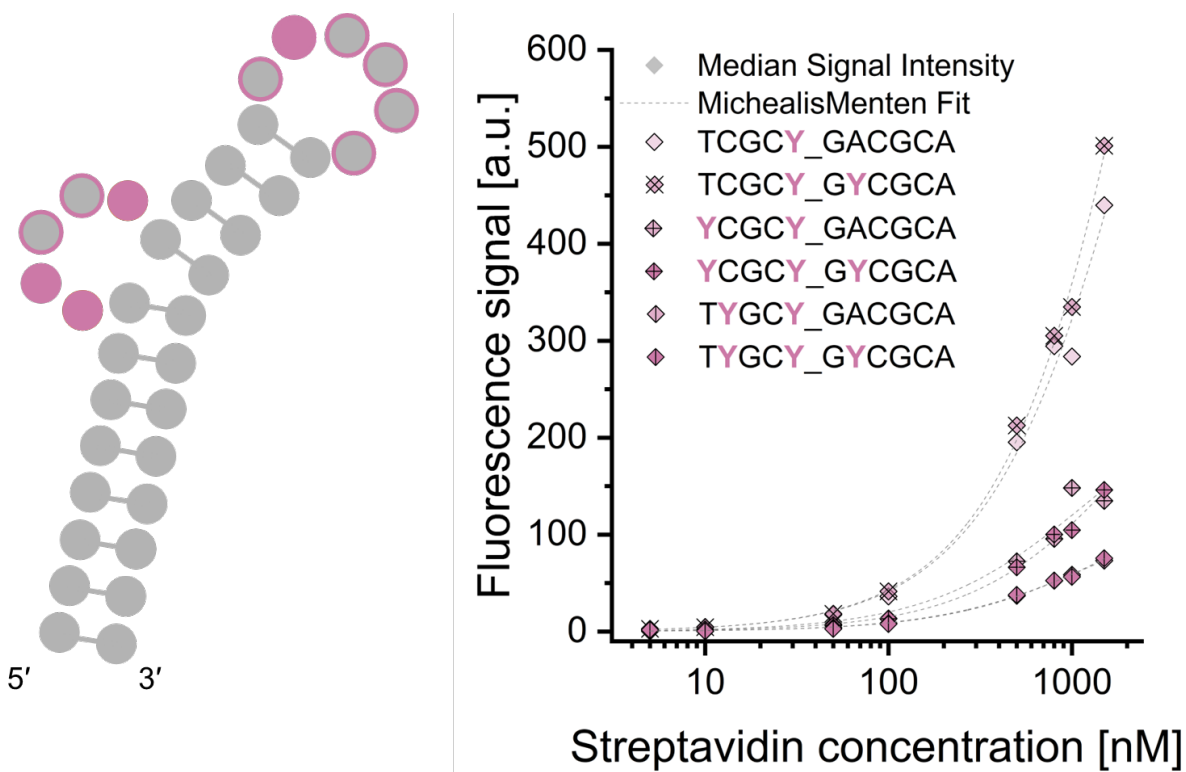


**Figure S7.** Assessment of dU-Tyr substitutions in the bulge and loop section of aptamer St-23-2. Left: Schematic representation of the predicted secondary structure with positions that have been permuted to dU-Tyr framed in pink, and those positions at which the introduction of dU-Tyr enabled protein binding filled with pink. Right: Fluorescence signal for binding of fluorescently labelled streptavidin at different concentrations to different variants of St-23-2 with site-specifically introduced dU-Tyr and hyperbolic fit to estimate binding affinity.